Defence Science Journal, Vol. 71, No. 2, March 2021, pp. 146-152, DOI : 10.14429/dsj.71.16127

Prediction of Moment Using a Modified Discrete Vortex Method in Ground Effect

Partha Mondal

Department of Space Engineering and Rocketry, Birla Institute of Technology Mesra, Ranchi - 835 215, India
E-mail: pmondal@gmail.com

ABSTRACT

The aerodynamics around a wing is modified when it comes near the ground. This is generally referred to as ground effect. In this work, a discrete vortex method based model which can predict two-dimensional (2D) ground effect from its free flight data is proposed. The required data in free flight could be generated either from high fidelity CFD solver or experiments. In this method, strength of the vortex distribution as obtained from discrete vortex based method is modified using a constrained optimisation procedure to match the free flight aerodynamic data. This vortex distribution is further modified due the presence of the ground. The efficacy of present model is demonstrated for predicting the moment of multi element airfoils in ground effect. The predicted aerodynamic coefficient in ground effect compares well with high fidelity CFD data.

Keywords: Ground effect; Panel method; Circulation; RANS simulation

NOMENCLATURE

C_D	Drag coefficient
C_L	Lift coefficient
C_M	Moment coefficient
c	Airfoil chord
D	Drag
D_{ref}	Reference drag
E_i	Error associated with panel i
G_{FF}	influence coefficients matrix in free flight
G_{GE}	influence coefficients matrix in ground effect
h	ground learance
I	$\sqrt{-1}$
K	$G_{GE}^{-1} G_{FF}$
L	Lift
L_{ref}	Reference lift
M_{ref}	Reference moment
M_∞	Freestream Mach number
Re	Freestream Reynolds number based on airfoil chord
R_i	Normal component of freestream velocity at panel i
U_∞	Freestream velocity
X	Force in the x direction
Y	Force in the y direction
Γ	Strength of vortex
Γ^∞	Strength of vortex in free flight
Γ'^∞	Modified strength of vortex in free flight
Γ'_{GE}	Predicted strength of vortex in ground effect
α	Angle of attack
ρ	Freestream density
y_+	Dimensionless wall distance

1 INTRODUCTION

The aerodynamics of a wing is referred to as ground effect when it operates near the ground. Aerodynamic coefficients get modified substantially from that of flight at higher altitudes. This phenomenon is referred to as "Ground Effect"[1–3]. During take-off and landing phase, an airplane flies near the ground with deployed high lift devices. This makes the flow physics more complex near the ground as compared to that in free flight. Ground effect is more crucial for the short take-off and landing (STOL) aircraft, particularly the naval version of fighter aircraft with more aggressive landing and take–off. It is also important for piloting the autonomous vehicles near ground. Ground effect is not restricted to take-off and landing of aircraft. It can also be seen in Wing in Ground (WIG) crafts, racing cars and WIG trains.[4–6] These vehicles utilize the advantages of ground effect for better efficiency. Both the experimental and numerical procedures can be used to perform the ground effect studies.

The studies on ground effect started as far back as the 1920s. Some of the early works are reported by Raymond[1] and Wieselsberger.[2] Raymond[1] investigated the ground effect by reflection method experimentally with different wings (Martin No. 2, R.A.F.15 Special and U.S.A.27) and observed an increase in L/D ratio as ground height is reduced (except at high α). Early analytical study by Wieselsbergers[2] showed the reduction in induced drag and increase in lift for mono and biplane configurations due to ground effect. In the review paper, Rozhdestvensky[4] surveyed the history, research and development of WIG craft technology. In the experimental investigation by moving ground plane method, a series of studies into single- and double–element inverted wings with end plates in ground effect were done by Zerihan & Zhang[5,8]. The main element has a modified General Aviation-Whitcomb (GAW) airfoil section. To apply the moving ground boundary condition, a moving belt rig was used. They have observed that for both single- and double-element wings, at large heights the downforce increases with decreasing in height. This downforce increases until it reaches maximum at some ground height and

Received : 14 July 2020, Revised : 23 November 2020
Accepted : 15 December 2020, Online published : 10 March 2021

then reduces with decreasing the height. The effect of Gurney flaps on the aerodynamic performances of airfoil was studied by Zerihan & Zhang[9] with same GAW wing section. Adding Gurney flap, lift is increased in ground effect as compared to free flight. Ahmed[10], *et al.* used moving belt system at ground to investigate the aerodynamic characteristics of NACA 4412 airfoil. Ranzenbach[7], *et al.* studied the flow field of an inverted two-element NACA 63_2-215 Mod B wing section in ground effect using fixed ground. They reported that a negative lift was increasingly developed as height decreased until a critical height reached from where lift increases with further reduction in height. Performance of 3-D wings for aero-levitation electric vehicle (AEV) in ground effect was studied numerically by Moon et al.[6] using Menter's k - ω/SST turbulence model. They concluded that there was a sizable corner flow separation at the junction of main and vertical (end plate) wing which was the primary cause of main wing L/D reduction for small wing span. Hsiun & Chen[11] investigated the effects of Reynolds number (*Re*), ground clearance and α on the aerodynamic characteristics of a NACA 4412 airfoil with standard k - ε turbulence model using stationary ground plane. They reported that C_L increases with the increase in *Re*. There was a large loss in lift at very close to the ground and they attributed this to the effect of ground boundary layer. Moryossef & Levy[12] simulated the flow field about a fixed airfoil and a heaving oscillating airfoil in close proximity to the ground at a single incidence. They conducted inviscid and turbulent flow simulations over Tyrell 026 wing section using Chimera grid technique. They showed that there are significant differences in the results for viscous and inviscid cases in extreme ground effect for fixed airfoil. And the result in inviscid case predicts more downforce than viscous flow. Zerihan & Zhang[13] performed a computational study for ground effect over an inverted, two-dimensional airfoil using moving wall boundary condition at the ground. They used Spalart-Allmaras and Menter k - ω turbulence models for the computation and compared the data with experimental results. The effect of an end plate and anhedral angle in ground effect was investigated by Lee[14], *et al.* to study the aerodynamics and stability of a wing with aspect–ratio of one. Qu[15], *et al.* investigated dynamic ground effect with NACA 4412 airfoil. They concluded that lift increases rapidly in dynamic ground effect as compared to static ground effect with decreasing ground height keeping α constant near the ground. The ground effect characteristics of a delta wing were investigated numerically by Qu[16], *et al.* They observed that there is increment in lift, drag as well as nose-down moment coefficients as ground clearance decreases. Dakhrabadi[17], *et al.* studied ground effect characteristics as well as stability of compound wing. Qin[18], *et al.* analysed the ground effect of canard configuration numerically. They reported that non-linear increment in lift, drag as well as nose-down pitching moment coefficients with reduction in ground clearance. Deng[19], *et al.* investigated ground effect aerodynamics of a wing with 30P30N 3-element high lift section numerically. They reported that lift, drag as well as nose-up pitching moment coefficients decrease with reduction in ground clearance.

The study of ground effect in conventional procedures is performed by keeping model at required height each time based on its ground clearance. Generally, in wind-tunnel experiments, the boundary condition at the ground is satisfied by a moving belt simulating the ground at a speed of freestream velocity. The high speed and vibrations associated with the moving belt make the experiments more cumbersome. On the other hand, the studies of the ground effect by numerical procedures need to generate grids for every ground clearance and incidence of the geometry. This requires more time and involvement in the numerical procedure for generating the data in ground effect. To alleviate these problems, a discrete vortex based model is proposed to predict the aerodynamic coefficients in ground effect. This model requires only CFD / experimental data at free flight. The efficacy of the model for predicting lift and drag in ground effect was well validated in the previous work[20,21]. In the present work, it is further extended to predict the coefficient of moment in ground effect only knowing the free flight aerodynamics. The predicted moment coefficient by the present model compares well with the high fidelity CFD data. The present model shows a lot of promise and it can be used as an effective tool in the early phase of design.

2. GENERALISED KUTTA-JOUKOWSKI THEOREM

Lift produced by a single vortex of strength Γ in a free stream with velocity U_∞ and density ρ is given by Kutta-Joukowski theorem[22] as $L = \rho U_\infty \Gamma$. But this relation is modified in the presence of other vortices which is generally referred to as Generalised Kutta-Joukowski (GKJ) theorem. References[20–22] provide some interesting reading for such type of flows, wherein the lift and drag forces experienced by a point vortex in the influence of other vortices are discussed. Here, we assume a vortex of strength Γ representing the body c_0 is placed at origin in a uniform flow of velocity U_∞ as shown in Fig. 1. To consider the effect of multiple vortices, N number of vortices each of strength Γ_k for k=1, N are placed in the vicinity of vortex Γ. Then, the complex potential associated with the above flow is given by,

$$\omega(z) = U_\infty z + \frac{I\Gamma}{2\pi}\ln(z) + \sum_{k=1}^{N}\frac{I\Gamma_k}{2\pi} ln(z - z_k) \qquad (1)$$

where $I = \sqrt{-1}$ and $z = x + Iy$. Now, we get complex velocity by differentiating the above equation with respect to z as,

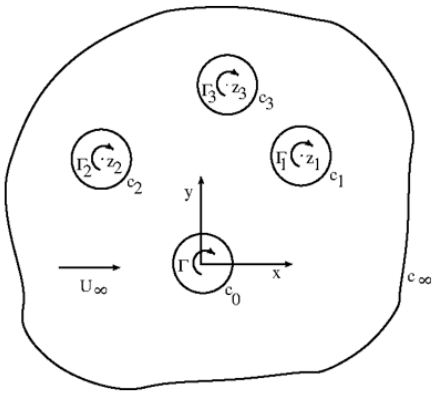

Figure 1. Nomenclature for the modified lift in the presence of other vortices.

$$\frac{d\omega}{dz} = U_\infty + \frac{I\Gamma}{2\pi z} + \sum_{k=1}^{N} \frac{I\Gamma_k}{2\pi(z - z_k)} \tag{2}$$

Now, Blasius integral theorem[22] states that the force acting on the body c_0 can be written as,

$$X - IY = \frac{I\rho}{2} \int_{c_0} \left(\frac{d\omega}{dz} \right)^2 dz \tag{3}$$

where the X and Y represent drag and lift forces respectively. The complex force on the body c_0 for an interaction problem with twin-vortex system is reported in reference.[22] A generalisation for the interaction problem with multiple vortices can be expressed as,

$$(X - IY)_{c_0} = (-I)\rho U_\infty \Gamma - \frac{\rho}{2} \sum_{k=1}^{N} \frac{\Gamma\Gamma_k}{\pi z_k} - \frac{\rho}{2} \sum_{k=1}^{N} \frac{\Gamma_k}{\pi} \sum_{\substack{n=1 \\ n \neq k}}^{N} \frac{\Gamma_n}{z_k - z_n} \tag{4}$$

Lift produced by an isolated vortex is seen in the first term. The remaining terms in the above equation are appearing due to the presence of other vortices. From the above relation, we can have the lift and drag forces acting on the body c_0 as,

$$L = \rho U_\infty \Gamma \left[1 + \sum_{k=1}^{N} \frac{\vec{q}_k^{\,0} . \vec{U}_\infty}{U_\infty^2} \right] \tag{5}$$

$$D = -\rho\Gamma \sum_{k=1}^{N} v_k^0 \tag{6}$$

where, $\vec{q}_k^{\,0}\left(u_k^0, v_k^0\right)$ is the velocity induced at origin by k^{th} vortex.

3. DISCRETE VORTEX METHOD

In the discrete vortex method (DVM),[22] camberline of the airfoil is discretised into N number of panels. The N vortex points are placed at the quarter chord point of these panels and zero normal flow boundary condition is satisfied at three–quarter point of each panel. The camberline of a multi-element airfoil is discretised into N number of panels as shown in Fig. 2. In case of ground effect, the ground boundary condition is satisfied using method of images.[22]

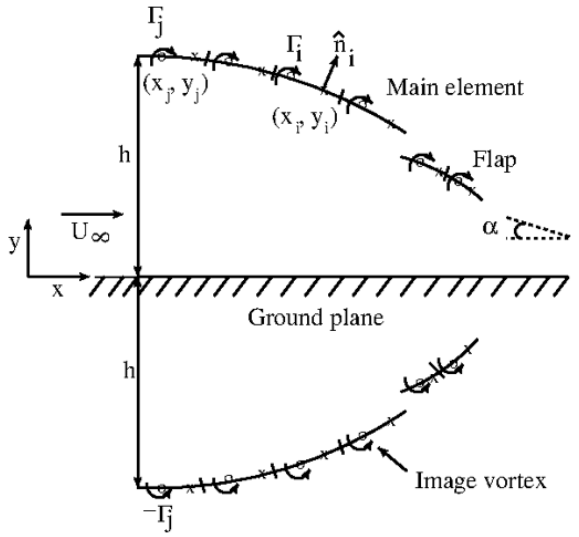

Figure 2. Representation of camberline of the main element and flap by discrete vortices in ground effect.

For this kind of flow, both the free stream camberline vortices and image vortex systems have contribution in the velocity field. The velocity components induced at the collocation point of i^{th} panel by the vortex at j^{th} panel and its image are,

$$[u - Iv]_{ij} = \frac{\Gamma_j}{2\pi\left[(x_i - x_j)^2 + (y_i - y_j)^2\right]} \left[(y_i - y_j) + I(x_i - x_j) \right] \tag{7}$$

$$[u - Iv]_{ij}^{image} = \frac{-\Gamma_j}{2\pi\left[(x_i - x_j)^2 + (y_i - y_j^{image})^2\right]} \left[(y_i - y_j^{image}) + I(x_i - x_j) \right] \tag{8}$$

where u and v are the velocity components in x and y directions, (x_i, y_i) represents the location of the collocation point of the i^{th} panel, (x_j, y_j) and $(x_j^{image}, y_j^{image}) = (x_j, -y_j)$ represent the location of vortex point of j^{th} panel and its image respectively. Now, zero normal velocity condition at the collocation point of i^{th} panel is,

$$\left[\sum_{j=1}^{N} \left[(u,v)_{ij} + (u,v)_{ij}^{image} \right] + (u_\infty, 0) \right] . \hat{n}_i = 0 \tag{9}$$

where, $\hat{n_i}(n_{xi}, n_{yi})$ represents unit normal at the collocation point of i^{th} panel. This will generate a linear system of equations as,

$$G_{GE}\Gamma = R \tag{10}$$

where G_{GE} is influence coefficients matrix with dimension $N \times N$. An element of the matrix

G_{GE} is defined as:

$$G_{GEij} = \left[(u,v)_{ij} + (u,v)_{ij}^{image} \right]_{\Gamma_j = 1} . \hat{n}_i \tag{11}$$

Also, an element of vector R can be written as,

$$R_i = -(u_\infty, 0) . \hat{n}_i \tag{12}$$

and the Γ can be expressed as $\Gamma = [\Gamma_1\ \Gamma_2 \ldots \Gamma_N]^T$. Solution of the above system of equations will give the discrete vortex distribution over the camber line in ground effect. Now, the lift and drag forces acting on the individual vortices are achieved by Eqns (5) and (6). Then sectional lift/drag is obtained by adding lift/drag forces felt by individual vortices over the camber line.

In case of free flight, the analysis is more simplified due the absence of ground. Here, the linear system of equations are expressed as,

$$G_{FF}\Gamma^\infty = R \tag{13}$$

where an element of G_{FF} is,

$$G_{FFij} = \left[(u,v)_{ij} \right]_{\Gamma_j = 1} . \hat{n}_i \tag{14}$$

4. PREDICTIVE MODEL

The objective of the present work is to develop a model which can predict the moment coefficient in ground effect by knowing its free fight data. This is performed by modifying the vortex strengths as obtained by classical DVM[22] to match the free flight aerodynamics. These required data in free flight could be generated either from CFD or experiment. A detailed discussion on this model is made in references[20,21] to predict lift and drag in ground effect. Therefore, the procedure to predict the moment will be presented here.

Moment Prediction

From the generalised Kutta-Joukowski theorem we can get the expression of lift and drag experienced by a vortex at point j as,

$$L_j = \rho U_\infty \Gamma_j^{'\infty} - \frac{\rho}{2}\sum_{\substack{k=1\\k\neq j}}^{N} \frac{\Gamma_j^{'\infty}\Gamma_k^{'\infty}}{\pi\left|z_k - z_j\right|^2}\left(y_k - y_j\right) \tag{15}$$

and

$$D_j = -\frac{\rho}{2}\sum_{\substack{k=1\\k\neq j}}^{N} \frac{\Gamma_j^{'\infty}\Gamma_k^{'\infty}}{\pi\left|z_k - z_j\right|^2}\left(x_k - x_j\right) \tag{16}$$

Moment can be obtained by summing up the elemental moments experienced by individual vortices. This elemental moment at a vortex point is due to the lift and drag experienced by that vortex as seen in generalised Kutta-Joukowski theorem. In the present analysis, reference point of moment is taken at origin. Therefore, expression of the moment can be written as,

$$M = -\sum_{j=1}^{N} x_j \left[\rho U_\infty \Gamma_j^{'\infty} - \frac{\rho}{2}\sum_{\substack{k=1\\k\neq j}}^{N} \frac{\Gamma_j^{'\infty}\Gamma_k^{'\infty}}{\pi\left|z_k - z_j\right|^2}\left(y_k - y_j\right)\right] - \sum_{j=1}^{N} y_j \frac{\rho}{2}\sum_{\substack{k=1\\k\neq j}}^{N} \frac{\Gamma_j^{'\infty}\Gamma_k^{'\infty}}{\pi\left|z_k - z_j\right|^2}\left(x_k - x_j\right) \tag{17}$$

In the conventional DVM, free flight Γ^{∞} distribution is obtained by satisfying normal velocity condition at the collocation points over the camber line. Here, in the present model, a modified vorticity distribution $\Gamma^{'\infty}$ is obtained along the camber line to satisfy the computed lift and moment with reference CFD / experimental data L_{ref} and M_{ref} in free flight. This is performed by relaxing the condition on normal velocity at each panel. Here, we specify an error E_i related to each panel,

$$E_i = \sum_{j=1}^{N} G_{FFij}\Gamma_j^{'\infty} - R_i \tag{18}$$

L_2 norm of the above error is minimised with keeping lift and moment as constraints,

$$C_1\left(\Gamma^{'\infty}\right) = \sum_{j}^{N} \rho U_\infty \Gamma_j^{'\infty} - L_{ref} = 0 \tag{19}$$

$$C_2\left(\Gamma^{'\infty}\right) = -\sum_{j=1}^{N} x_j \left[\rho U_\infty \Gamma_j^{'\infty} - \frac{\rho}{2}\sum_{\substack{k=1\\k\neq j}}^{N} \frac{\Gamma_j^{'\infty}\Gamma_k^{'\infty}}{\pi\left|z_k - z_j\right|^2}\left(y_k - y_j\right)\right] - \sum_{j=1}^{N} y_j \frac{\rho}{2}\sum_{\substack{k=1\\k\neq j}}^{N} \frac{\Gamma_j^{'\infty}\Gamma_k^{'\infty}}{\pi\left|z_k - z_j\right|^2}\left(x_k - x_j\right) - M_{ref} = 0 \tag{20}$$

Now, $\sum E_j^2 - \lambda_1 C_1 - \lambda_2 C_2$ is minimised subject to constraints on lift and moment, where $\lambda_1$and λ_2 are Lagrange multipliers.

Noting Equations (10) and (13), we can write,

$$G_{GE}\Gamma_{GE} = G_{FF}\Gamma^{\infty} = R \tag{21}$$

$$\Gamma_{GE} = K\Gamma^{\infty} \tag{22}$$

where, K is defined as $K = G_{GE}^{-1}\, G_{FF}$. This suggests that the modified Γ distribution in ground effect can be obtained as,

$$\Gamma_{GE}^{'} = K\Gamma^{'\infty} \tag{23}$$

Having obtained modified vortex ($\Gamma^{'\infty}$) distribution in free flight, the Γ distribution in the influence of ground plane can be calculated from Eqn (23). This modified Γ can be used to evaluate the moment in ground effect.

5. RESULTS AND DISCUSSION

5.1 Validation of the Flow Solver

The present model requires free flight aerodynamic data, obtained either by CFD / experiment, to predict the ground effect. To validate the model, data corresponding to various ground clearances are also required. In the absence of complete set of standard data in open literature in free flight and ground effect, an in-house code is used to generate the required data. Therefore, the present RANS solver is validated before it is used for validating the proposed model. The present in-house solver is based on cell center finite volume method. It employs on unstructured data and is capable of handling complex geometries. In the present solver, Roe[23] flux formula has been used for the computation of inviscid fluxes. Venkatakrishnan limiter[24] is used to preserve the monotonicity near the discontinuities by limiting the gradients of the flow variables. Green-Gauss procedure[25] popularly known as diamond path reconstruction is used to compute the gradients. Convergence acceleration is attained by using Symmetric-Gauss-Seidel (SGS) implicit relaxation procedure.[26] Spalart-Allmaras turbulence model[27] is used to compute the eddy viscosity. Moving wall has been used to satisfy the boundary condition at the ground plane.

The present solver is validated with a standard test case for the turbulent flow over McDonnell Douglas Aerospace (MDA) 3-element airfoil[28,29]. This geometry is 30P-30N configuration with both the flap and slat deflected at 30^0.The flow condition for this case is $M_\infty = 0.2$, $Re = 5 \times 10^6$ and $\alpha = 8.12^0$. A hybrid unstructured grid with number of volumes around 333000 is generated using commercial tool GAMBIT for the simulation. The grid around this airfoil is shown in Fig. 3(a). The y_+ of the first grid point located off the wall is less than 1. Here, y_+ is called dimensionless wall distance and it is defined as $y_+ = \frac{yu_*}{\nu}$, where y, u_* and ν are the wall distance, friction velocity and kinematic viscosity respectively. Pressure distribution over the airfoil compares well with the experimental data[29] as shown in Fig. 3(b). The experiments were conducted in the NASA Langley Low Turbulence Pressure Tunnel (LTPT) with MDA 3-element 30P-30N configuration. The flow features over the multi-element airfoil can be he observed in Mach and pressure contours as shown in Figs. 3(c) and 3(d) respectively. Table 1 shows the computed and standard values of aerodynamic coefficients. The pitching moment was computed with respect to the quarter chord point of the airfoil. It can be observed that the computed aerodynamic coefficients compare well with the experimental[29] as well as other standard numerical data[30] available in the literature. This shows the ability and usefulness of the present solver to validate the proposed ground effect model.

Table 1. Validation of free flight lift (C_L), drag (C_D) and moment (C_M) co-efficients for a MDA 3-element high lift section with experimental data (M_∞ = 0.2, Re = 5 × 10^6, α = 8.12°)

Configuration	Experiment[29]			Present CFD			Mavriplis/ Klausmeyer in Ref.[30]		Rogers in Ref.[30]
	C_L	C_D	C_M	C_L	C_D	C_M	C_L	C_D	C_M
MDA 3-element	3.0841	0.0361	-0.5701	3.3142	0.0418	-0.6180	3.2789	0.0434	-0.6097

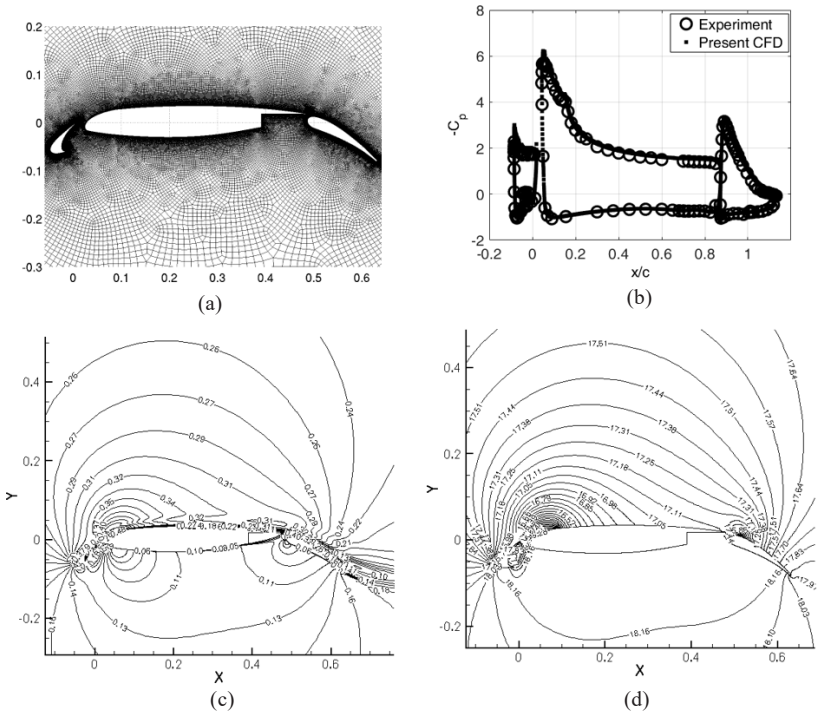

Figure 3. MDA 3- element airfoil in free flight at α = 8.12^0 (M_∞ = 0.2, Re = 5 × 10^6) (a) Grid, (b) C_p distribution, (c) Mach contours, and (d) Pressure contours.

5.2 Moment Prediction in Ground Effect

The procedure demonstrated above is applied on multi-element airfoils in ground effect. The geometries considered for the present analysis are MDA 3-element and National High Lift Programme (NHLP)-2-D 3-element airfoils. The free flight reference data required for the present model are generated using high fidelity RANS solver. All the grids used for the present computation are wall resolved and the y+ of the first point off the wall is less than 1. In the present analysis, moment is calculated about the leading edge of the main element. Also, the ground clearance is defined from the leading edge of the main element.

In the first case, turbulent flow over MDA 3-element airfoil with free stream condition M_∞ = 0.2, Re = 5 × 10^6 and α = 8.12^0 is considered. The grid used for the simulation is hybrid unstructured as shown in Fig. 4(a). The number of cells about 350000 have been generated in the computational domain for h/c = 0.4. Predicted moment coefficient by the present model is compared with the conventional DVM and CFD data at different ground heights as shown in Fig. 4(b). C_M computed by the present model compares well with the CFD data. The maximum difference in the predicted value is found to be 2.47% at h/c = 0.4. The flowfield over the airfoil at h/c = 0.4 is shown in Mach and pressure contours as indicated by Figs. 4(c) and 4(d) respectively. Wake of an element convects directly over the trailing element and there exists a large wake behind the flap. At low ground height, this wake interacts with the ground and makes the flow more complex. In the present simulation, moving wall boundary condition is implemented to simulate the ground plane. Therefore, Mach number on the ground plane is equal to free stream value. Due to the ram effect, Mach number is small in between the ground plane and airfoil. This can be observed in the Mach contours in Fig. 4(c). Pressure is increased in between the airfoil and ground plane due to ram effect. This high pressure remains almost constant over the bottom surface of main element and flap as seen in Fig. 4(d).

To validate the present model, another exercise is performed with NHLP-2-D 3-element airfoil. A free stream condition with M_∞ = 0.197, Re = 3.52 × 10^6 and α = 10^0 involves a standard test case. Same flow condition is also used for the ground effect study. A zoomed view of the grid, with number of cells about 176000, near the airfoil is shown in Fig. 5(a) for ground clearance h/c=0.4.

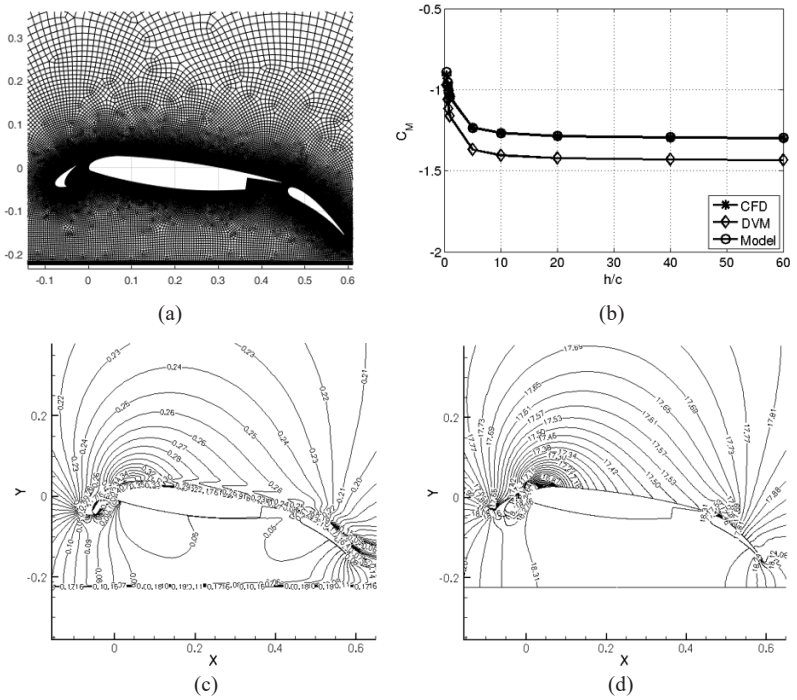

Figure 4. MDA 3-element airfoil in ground effect at α = 8.12^0 (M_∞ = 0.2, Re = 5 × 10^6): (a) Grid at h/c = 0.4, (b) Comparison of C_M, (c) Mach contours at h/c = 0.4, and (d) Pressure contours at h/c = 0.4.

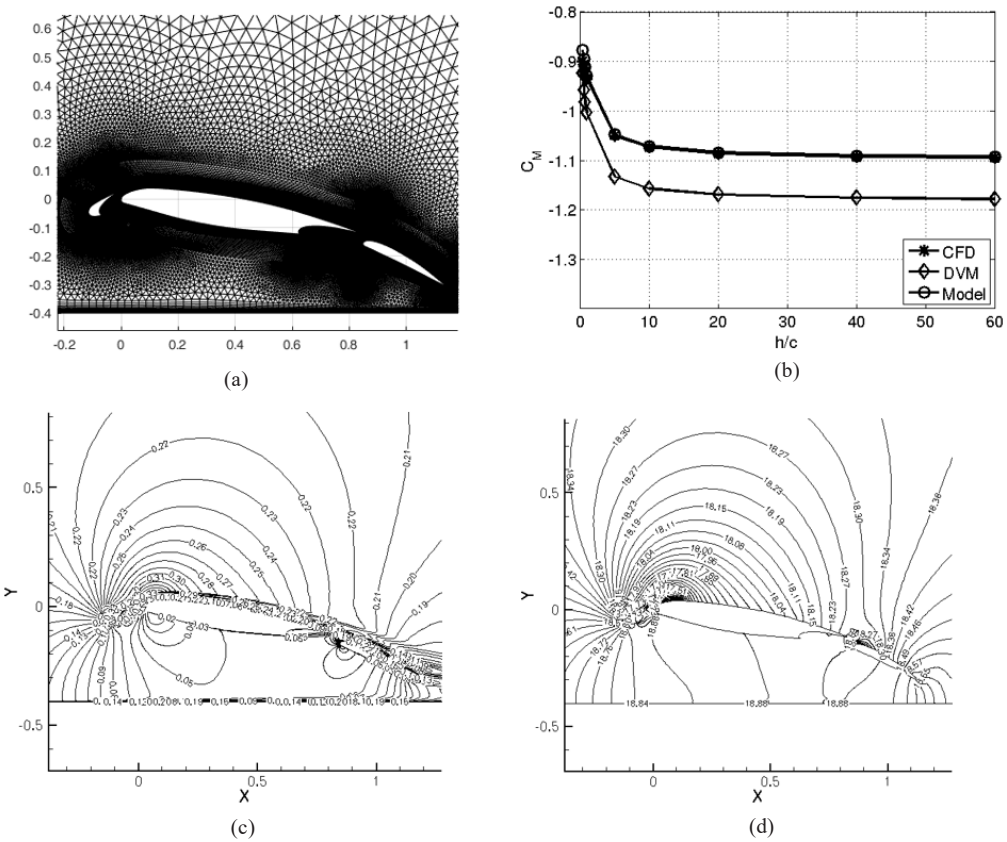

Figure 5. NHLP-2-D 3-element airfoil in ground effect at α = 10⁰ (M_∞ = 0.197, *Re* = 3.52 × 10⁶) (a) Grid at h/c = 0.4, (b) Comparison of C_M, (c) Mach contours at h/c = 0.4, and (d) Pressure contours at h/c = 0.4.

The moment coefficients predicted by the present model for various ground clearances are compared with data as obtained from CFD in Fig. 5(b). In this case also, there is an excellent match between the C_M computed with the model and CFD data, and a maximum deviation in C_M is found to be 2.44% at ground clearance (h/c) of 0.4. Also, Mach and pressure contours at h/c = 0.4 for this geometry are shown in Figs. 5(c) and 5(d) respectively. The flow features of this geometry are similar to flow over MDA 3-element airfoil in ground effect as discussed above. Therefore, the cases presented clearly demonstrate the ability of the present model to predict the moment coefficient in 2-D ground effect.

6. CONCLUSIONS

A modified discrete vortex method for ground effect studies has been established. In this procedure, vortex distribution as obtained by the discrete vortex method is modified using a constrained optimisation procedure to match the free flight data. The free flight data could be generated using high fidelity CFD solver or experiment. The vortex distribution is further modified due to the presence of ground plane in ground effect. The work also demonstrates ability of the model to predict moment coefficient of high-lift multi-element configurations in ground effect. The predicted results compare well with the standard CFD data and demonstrate the efficacy of the present methodology. This can be considered as a very useful tool in the early phase of the design process.

REFERENCES

1. Raymond, A. E. Ground influence on airfoils. NACA TN No. 67, December, 1921.
2. Wieselsberger, C. Wing resistance near the ground. NACA TM No. 77, April, 1922.
3. Houghton, E.L. & Carpenter, P.W. Aerodynamics for Engineering Students. Butterworth- Heinemann, 2003.
4. Rozhdestvensky, K. V. Wing–in–ground effect vehicles. *Progress in Aerospace Sciences*, 2006, **42**, 211–283. doi: 10.1016/j.paerosci.2006.10.001
5. Zhang, X. & Zerihan, J. Aerodynamics of a double-element wing in ground effect. *AIAA Journal*, 2003, **41**(6), 1007–1016. doi: 10.2514/2.2057
6. Moon, Y. J.; Oh, H. & Seo, J. Aerodynamic investigation of three-dimensional wings in ground effect for aero-levitation electric vehicle. *Aerospace Science and Technology*, 2005, **9**(6), 485–494. doi: 10.1016/j.ast.2005.01.005
7. Ranzenbach, R.; Barlow, J. B. & Diaz, R. H. Multi-element airfoil in ground effect–an experimental and computational study. AIAA Paper 97–2238, 1997.
8. Zerihan, J. & Zhang, X. Aerodynamics of a single element wing in ground effect. *Journal of Aircraft*, 2000, **37**(6), 1058–1064. doi: 10.2514/2.2711
9. Zerihan, J. & Zhang, X. Aerodynamics of of Gurney flaps on a wing in ground effect. *AIAA Journal*, 2001, **39**(5),

772–780.
doi: 10.2514/2.1396

10. Ahmed, M. R.; Takasaki, T. & Kohama, Y., H. Experiments on the aerodynamics of a cambered airfoil in ground effect. AIAA Paper 2006–258, 2006.
doi: 10.2514/6.2006-258
11. Hsiun, C. & Chen, C. Aerodynamic Characteristics of a Two-Dimensional Airfoil with Ground Effect. *Journal of Aircraft*, 1996, **33**(2), 386–392.
doi: 10.2514/3.46949
12. Moryossef, Y. & Levy, Y. Effect of oscillations on airfoils in close proximity to the ground. *AIAA Journal*, 2004, **42**(9), 1755–1764.
doi: 10.2514/1.6380
13. Zerihan, J. & Zhang, X. A single element wing in ground effect; comparisons of experiments and computation. AIAA Paper 2001-0423, 2001.
14. Lee, J.; Han, C. & Bae, C.-H. Influence of wing configurations on aerodynamic character- istics of wings in ground effect. *Journal of Aircraft*, 2010, **47**(3), 1030–1040.
doi: 10.2514/1.46703
15. Qu, Q.; Jia, X.; Wang, W.; Liu, P. & Agarwal, R. K. Numerical study of the aerodynamics of a NACA 4412 airfoil in dynamic ground effect. *Aerospace Science and Technology*, 2014, **38**, 56–63.
doi: 10.1016/j.ast.2014.07.016
16. Qu, Q.; Lu, Z.; Guo, H.; Liu, P. & Agarwal, R. K. Numerical Investigation of the Aero- dynamics of a Delta Wing in Ground Effect. *Journal of Aircraft*, 2015, **52**(1), 329–340.
doi: 10.2514/1.C032735
17. Dakhrabadi, M. T. & Seif, M. S. Influence of main and outer wings on aerodynamic charac- teristics of compound wing-in-ground effect. *Aerospace Science and Technology*, 2016, **55**, 177–188.
doi: 10.1016/j.ast.2016.06.002
18. Qin, Y.; Liu, P.; Qu, Q. & Hu, T. Wing/canard interference of a close-coupled canard configuration in static ground effect. *Aerospace Science and Technology*, 2017, **69**, 60–75.
doi: 10.1016/j.ast.2017.06.012
19. Deng, N.; Qu, Q. & Agarwal, R. K. Numerical Study of the Aerodynamics of a Rectangular Multi-Element Wing in Ground Effect. AIAA Paper 2018-4115, 2018.
doi: 10.2514/6.2018-4115
20. Mondal, P. Wing in Ground Effect. Ph.D. Thesis, Department of Aerospace Engineering, Indian Institute of Science, Bangalore, 2014.
21. Mondal, P. & Balakrishnan, N. Discrete Vortex Method-Based Model for Ground-Effect Studies. *AIAA Journal*, 2014, **52**(12), 2817–2828.
doi: 10.2514/1.J052920
22. Joseph Katz & Allen Plotkin. Low-Speed Aerodynamics. Cambridge University Press, 2001.
23. Roe, P. L. Approximate Riemann solvers, parameter vectors and difference schemes. *Journal of Computational Physics*, 1981, **43**, 357–372.
doi: 10.1016/0021-9991(81)90128-5
24. Venkatakrishnan, V. Convergence to Steady State Solutions of the Euler Equations on Unstructured Grids with Limiters. *Journal of Computational Physics*, 1995, **118**, 120–130.
doi: 10.1006/jcph.1995.1084
25. Jawahar, P. & Kamath, H. A high resolution procedure for Euler and Navier–Stokes computations on unstructured grids. *Journal of Computational Physics*, 2000, **164**, 165–203.
doi: 10.1006/jcph.2000.6596
26. Shende, N. V. & Balakrishnan, N. New Migratory Memory Algorithm for Implicit Finite Volume Solvers. *AIAA Journal*, 2004, **42**(9), 1863–1870.
doi: 10.2514/1.8969
27. Spalart, P. R. & Allmaras, S. R. A One-Equation Turbulence Model for Aerodynamic Flows. AIAA Paper 92–0439, 1992.
doi: 10.2514/6.1992-439
28. Rumsey, C. L. & Ying, S. X. Prediction of high lift: review of present CFD capability. *Progress in Aerospace Sciences*, 2002, **38**, 145–180.
doi: 10.1016/S0376-0421(02)00003-9
29. Private communication with C. Rumsey, Senior Research Scientist, NASA Langley Research Center, Hampton, VA, 2008.
30. Klausmeyer, S. M. & Lin, J. C. Comparative Results From a CFD Challenge Over a 2–D Three–Element High–Lift Airfoil. NASA TM 112858, May 1997.

CONTRIBUTOR

Dr Partha Mondal obtained his PhD in Aerospace Engineering from Indian Institute of Science, Bangalore. He is presently working as Assistant Professor at the Department of Space Engineering and Rocketry, BIT Mesra, Ranchi. His areas of research include: Aerodynamics, Computational Fluid Dynamics.